Silicon light-emitting device for fast optical interconnect and fast sensing applications in the GHz frequency range in standard IC technology

KAIKAI XU[a,*], KINGSLEY A. OGUDO[b], LUKAS W. SNYMAN[b], HERZL AHARONI[c]
[a]*State Key Laboratory of Electronic Thin Films and Integrated Devices, University of Electronic Science and Technology of China, China*
[b]*Department of Electrical and Mining Engineering, University of South Africa, Florida Campus, South Africa*
[c]*Department of Electrical and Computer Engineering, Ben- Gurion University, Beer-Sheva, Israel*

A monolithically integrated silicon light-emitting device with visible light emission (400–900 nm) is presented to realize sensing application in high frequency on the CMOS platform.

(Received May 20, 2016; accepted April 6, 2017)

Keywords: Silicon, Optoelectronics, Frequency, Interconnect

1. Introduction

The fabrication of high frequency single crystal silicon light-emitting devices (Si-LEDs) is important for the integration of photonic and electronic components on the same Si substrate using the standard complementary metal oxide semiconductor (CMOS) process technology and because the fabrication possibilities of all-silicon optoelectronic integrated circuits (OEIC's) [1]. From recent published work it is derived that these devices can also play a significant role in the development of sensing application in GHz as well as for the application of optical interconnects for optoelectronic integrated circuits [2].

The fact that reversed biased silicon PN junctions which operate in the breakdown mode can emit light is known since 1955 as a physical phenomena. In order to produce practical Si-LEDs our research is focused on two main subjects: (a) studying in PN junctions the affect of their structural parameters on their light generation capabilities, and; (b) providing high functional diversification of CMOS integrated circuits with high-frequency capabilities of the order of GHz, by exploring the possibilities of monolithically integrating them with newly developed Si-LEDs having a third terminal, which control their light output by low power electrical input, facilitating wide range modulation of light signals intensity, enabling significantly higher rate optoelectronic signal processing operations through optical coupling between the transistors, instead of the presently employed metallurgical coupling which are associated with RC delays limiting signal processing rate.

2. Electroluminescence from Silicon PN Avalanching junctions devices

In PN junctions which are operated in the reverse bias avalanche mode, hot carriers (both electrons and holes) are accelerated in the high electric field E (about 5×10^5 V/m) of the depletion region gaining high energy which is transferred by collision to the silicon lattice atoms, creating excess electron-hole pairs by impact ionization with the silicon atoms. The above process proceeds in an accumulative fashion, by progressively multiplying the excess carriers number in a similar fashion, giving rise to a creation of the high density of excess carriers in and around the depletion region. These excess carriers occupy a range of high energy levels in the band diagram. Light is generated almost simultaneously as a result of the subsequent energy relaxation of the above excess carriers by a recombination processes giving rise to a wide (400–900 nm) emitted spectra [3].

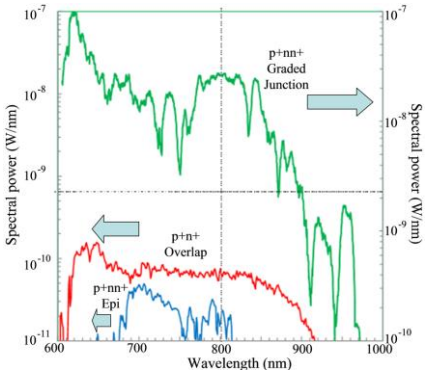

Fig. 1. Normalized electroluminescence spectra of three different types of Si PN junctions

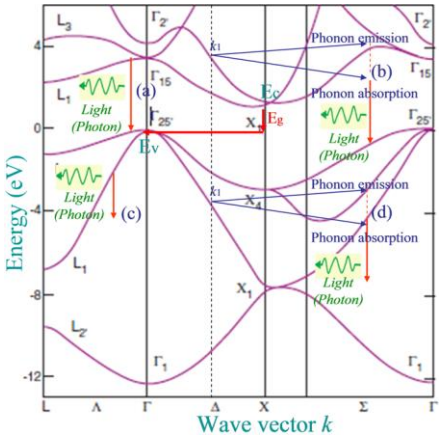

Fig. 2. Si band structure to interpret the four different transitional processes: (a) inter-band direct transition; (b) inter-band indirect transition; (c) intra-band direct transition; (d) intra-band indirect transition

Fig. 1 shows the normalized electroluminescence spectra of three different types of PN junctions. It is noted that they have the same emitting wavelength range but different power conversion efficiencies according to their different structures, indicating that the overall light intensity emission can be improved by structural design. In this example these efficiencies shown to be significantly improved from 10^{-9} and 10^{-8}, respectively, by a factor of about 10^3 by utilizing special device structures and favoring specific photonic yield processes [4].

The mechanism governing the formation of the above spectra is not fully established yet. However, there are four major types of possible optical radiation mechanisms which are summarized in Fig. 2. The dominant emission peaks of 650 nm and 550 nm (within the visible range) indeed are observed in the emission spectra in Fig. 1, and these peaks are directly related to energy-to-photon conversion processes. Especially, the 650 nm wavelength occurs mainly through a process of phonon assisted carrier recombination.

3. Transient analysis of P^+N junction with controlling gate

Fig. 3 shows an MOS-like Si-LED which is composed from P^+N drain junction, and an insulated gate which serves as a third light intensity controlling terminal by applying gate voltage V_g. Changes in V_g cause electric field modulation within the junction depletion layer (simulated in Fig. 4) and hence effect the generation-recombination process. The resulting generated light is emitted mainly via the transparent gate.

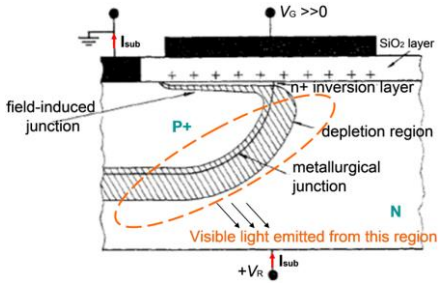

Fig. 3. Reverse-biased P^+N junction covered by an insulated gate, and operated in the breakdown mode. The depletion region width and electric field are modified by applying a voltage V_g to the gate terminal, resulting light intensity modulation

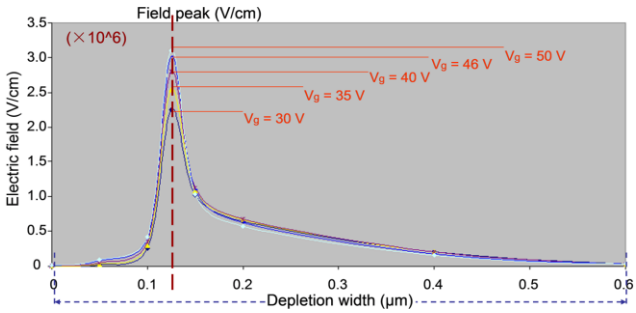

Fig. 4. Electric field distribution in a depletion region of the p^+n abrupt junction gate controlled-diode, at different gate voltages V_g. .(calculated by the integration of Poisson equation)

Fig. 5, presents the dependence of the integrated light output emission power W_{opt} (over the whole generated spectrum), on the gate voltage V_g, for three different fixed substrate voltages V_{sub}. It is observed that as a gate voltage V_g exceeds certain gate threshold, a high rate (dW_{opt}/dV_g) of increase in the optical output takes place, indicating the sensitive control capabilities of the light emission, enabling light intensity modulation by either analog or digital electrical signals applied to the gate terminal. This dependence can also serve as a tool for channel condition determination in MOSFETs [5], since the changes of V_g affect the changes in the channel properties(such as changes from strong to week inversion etc.) [6].

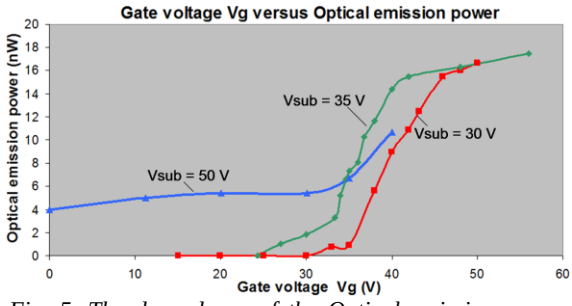

Fig. 5. The dependence of the Optical emission power W_{opt} versus Gate voltage V_g, at different substrate voltages: V_{sub} = 50 V, V_{sub} = 35 V, and V_{sub} = 30 V. Both source and drain are connected to the ground. The gate voltage V_g is a varied while the reverse bias of the "p^+ Source and Drain to n-Substrate" junctions is equal to V_{sub}

Finally, the switching speed for a reverse-biased p-n junction is closely related to the transit time of the excess minority carriers generated in the depletion region. It is estimated as follows: the escape time τ_{th} by thermionic emission of the hot carriers in the high electric field of the depletion region is of the form:

$$\frac{1}{\tau_{th}} = \frac{1}{L}\sqrt{\frac{kT}{2\pi m_e^*}}\exp\left(-\frac{\Delta E}{kT_e}\right) \quad (1)$$

where L is the quantum-well width, T_e is the effective temperature of the carrier, m^* is the carrier effective mass, and the energy barrier height ΔE strongly depends on the local electrical field [7]. It is worth noting that the field peak in the p-n junction depletion region (Fig. 4) is about 3×10^6 V/cm. For these values τ_{th} is evaluated to be 7.5 ps for a zero electric field, and less than 0.1 ps for the electric field of 3×10^6 V/cm. For such a high field, the saturated drift velocity of the electrons is 10^7 cm/s. Similarly, the transit time of hot carriers through a depletion region of ~0.6 μm will be in about 6 ps, thus leading to a intrinsic response speed in excess of 10 GHz. The modulation speed is reasonably in good agreement with the experimentally achieved speed of 350 MHz [8]. Since the gate-controlled diode is operated in breakdown condition, any other expected effects in terms of reliability should be taken into account [9]. A novel method for sensing application in GHz frequency range in standard IC technology is presented for creating modern sensing systems with integrated silicon light sources [10].

4. Conclusion

Our work as presented here-realized in practice the fabrication of Si-LEDs using the standard conventional fully industrialized IC CMOS technology “as is” without any adaptation by three terminal gate controlled MOS-like Si-LED, with potentially extremely high switching speeds. These devices can find very interesting applications for various sensing and interconnect applications in futuristic CMOS photonic related IC’s. The gate controlled inversion layer modulates the depletion layer width and electric field and hence modulate the light emission intensity. The light emission zones can be positioned nearby transparent wave-guiding structures. This approach enables Si-LEDs fabrication in the same production lines of the presently existing IC industry. The result is that the yield, reliability, and price of the above Si-LEDs are the same as the other Si devices integrated on the same chip, thus for sensing application in GHz frequency range in standard IC technology.

Acknowledgement

This work is supported by the Natural Science Foundation of China under Contract 61674001, the National Research Foundation Rated Researcher Incentive Funding under Contract IFR2011033100025, Department of Science and Technology of Sichuan Province under Contract 2016JY0217, the Open Foundation of State Key Laboratory of Electronic Thin Films and Integrated Devices under Contract KFJJ201508, and the Open Foundation of Defense Key Disciplines Lab of Novel Micro-nano Devices and System Technology (Chongqing University).

References

[1] L. Snyman, M. du Plessis, E. Seevinck, H. Aharoni, IEEE Electron Device Lett. **20**(12), 614 (1999).
[2] K. Ogudo, D. Schmieder, D. Foty, L. Snyman, J. Micro/Nanolithograph, Microfabrication, Microsyst. **12**(1), 013015 (2013).
[3] L. Snyman, K. Xu, J. Polleux, K. Ogudo, C. Viana, IEEE J. Quantum Electron. **51**(6), 3200110 (2015).
[4] K. Xu, K. Ogudo, J. Polleux, C. Viana, Z. Ma. Z. Li, Q. Yu, G. Li, L. Snyman, LEUKOS, the Journal of the Illuminating Engineering Society. **12**(4), 203 (2016).
[5] K. Xu, Q. Yu, G. Li, IEEE J. Quantum Electron. **51**(8), 3000106 (2015).
[6] K. Xu, N. Ning, K. Ogudo, J. Polleux, Q. Yu, L. Snyman, Proc SPIE **9667**, International Workshop on Thin Films for Electronics, Electro-Optics, Energy, and Sensors, 966702, (2015).
[7] K. Xu, Z. Zhang, Q. Yu, Z. Wen, IEEE J. Disp. Technol. **12**(2), 115 (2016).
[8] D. Marris, E. Cassan, L. Vivien, J. Appl. Phys. **96**(11), 6109 (2004).
[9] J. McKendry, R. Green, A. Kelly, Z. Gong, B. Guilhabert, D. Massoubre, E. Gu, M. Dawson, IEEE Photon. Tech. Lett. **22**(18), 1346 (2010).
[10] S. Tan, J. Teo, D. Isakov, D. Chan, L. Koh, C. Chua, J. Phang, in Proc. 15th IEEE Int. Symp. Physical and Analysis of Integr. Circuits 1-5 (2008).

*Corresponding author: kaikaix@uestc.edu.cn